B. PISAREK*#, C. RAPIEJKO*, T. PACYNIAK*

EFFECT OF INTENSIVE COOLING OF ALLOY AC-AlSi7Mg WITH ALLOY ADDITIONS ON MICROSTRUCTURE AND MECHANICAL PROPERTIES

The work presents results of the investigations of effect of intensive cooling of alloy AC-AlSi7Mg with alloy additions on microstructure and mechanical properties of the obtained casts. The experimental casts were made in ceramic molds preliminarily heated to 180°C, into which AC-AlSi7Mg with alloy additions was poured. Within implementation of the research, a comparison was made of the microstructure and mechanical properties of the casts obtained in ceramic molds cooled at ambient temperature and the ones intensively cooled in a cooling liquid. Kinetics and dynamics thermal effects recorded by the TDA method were compared. Metallographic tests were performed with the use of optical microscope and strength properties of the obtained casts were examined: UTS, Elongation and HB hardness.

Keywords: solidification process, aluminum alloy, alloy additions, intensive cooling, mechanical properties

1. Introduction

Aluminum alloys due to good castability, low thermal expansion and relatively good mechanical properties find application on cast parts of machines and devices in automotive, aerospace and space industries [1,2]. Aluminum alloy castings, depending on the production technology and heat treatment, have different mechanical properties, which in some applications are too low. Improvement of mechanical properties of castings of aluminum and silicon alloys is obtained as a result of appropriate treatments on a liquid alloy such as: modification of morphology of silicon eutectic particles [3], introduction of alloy additives [4,5], and in the case of manufacturing of castings by: application of intensive cooling [6,7] or heat treatment [8] castings.

The Department of Materials Engineering and Production Systems, Lodz University of Technology (KTMiSP PŁ), has realized, within the Applied Studies Program, the project „Elaboration of innovative technologies of producing complex construction high quality precisions casts from light metal alloys". The project was implemented within the frames of a consortium, in which KTMiSP PŁ was one of its members. The practical aim of the project was to develop innovative production technologies of precision casts in the investment casting method from the newly-elaborated aluminum alloys. The technology is to be an alternative for the pressure casting processes for products of high technical and economical effectiveness in small and medium lot production. One of the project tasks realized at KTMiSP PŁ was to examine the effect of physical and chemical state of the liquid metal on microstructure and mechanical properties of the experimental casts. The work is a continuation of research concerning improved mechanical properties of aluminum alloy AC-AlSi7Mg, which was described in the publication (B.P. Pisarek et al.) [9]. The task includes application of intensive cooling of the mold and its effect on microstructure and mechanical properties of the elaborated aluminum alloys.

2. Test methodology

The investigations of the effect of intensive cooling of the ceramic mold on mechanical properties were performed for the aluminum alloys AC-AlSi7Mg0.3 with the addition of 4% Cu, 2.5% Ni and 0.1% of each: Cr, V, Mo, W; (AC-AlSi7Mg+) [9]. The alloy was melted in an induction furnace, in AC20 – type crucible made of silicon carbide. The alloy additions were introduced in form of master alloys: AlCu50/50, AlNi20, AlCr15 and AlV10, as well as technically pure metals: Si, Mg, W and Mo. The alloy was modified with Sr (AlSr10), and next refined with N_2 for 5 min. The casting temperature was 750°C.

For construction of the gating system, models of the following components, used at the Labour Cooperative ARMATURA (Lodz, Poland), were applied: the pouring basin, the runners and the gates WD25 and WD45. The ceramic mold for the TDA tests and for production of strength samples – produced at the Labour Cooperative ARMATURA – consists of seven coatings applied in mixers and a fluidizer. Each coating was created as a result

*   LODZ UNIVERSITY OF TECHNOLOGY, DEPARTMENT OF MATERIALS ENGINEERING AND PRODUCTION SYSTEMS, 1/15 STEFANOWSKIEGO STR., 90-924 ŁÓDŹ, POLAND

Corresponding author: boguslaw.pisarek@p.lodz.pl

of applying a binder on a wax model, and next covering the latter with quartz sand of a specific granularity. The configuration and type of applied coatings were discussed in the work [10]. The following step in the mold preparation process consisted in annealing at 800°C in a tunnel furnace, and next cooling of the mold to 180°C. The molds prepared in this way were filled with the liquid alloy's, after solidification of about 30% of the alloy volume in a random micro-volume of the casts, were submerged in a cooling liquid at the rate of V_{tb} = 0.08 m/s (Fig. 1). As the cooling liquid a 20% solution of Polihartenol-E8 in water was used, at the ambient temperature t_{at} = 20°C.
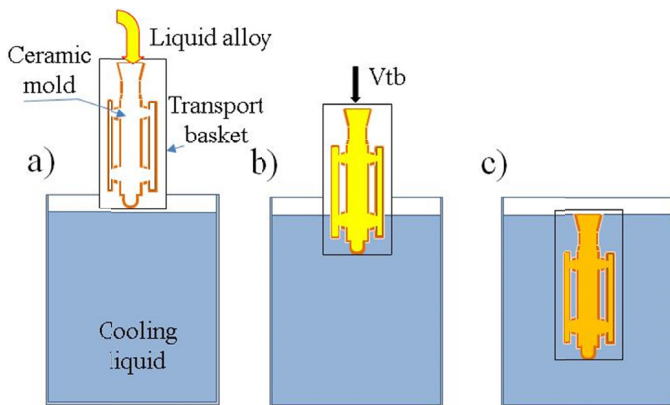

Fig. 1. Steps of alloy pouring (a) and intensive cooling of the ceramic mold (b, c); V_{tb} = 0.08 m/s

The examinations of the process of solidification and crystallization of alloy AC-AlSi7Mg+ were performed in specially designed and produced ceramic samplers ATD10C-PŁ with the use of the TDA method's. Construction of the samplers and the schematics of the TDA method testing station for the alloys cooling at ambient temperature have been described in the work [10]. The schematics of the TDA method's testing station of the alloys intensively cooled in a cooling liquid have been discussed in the work [11].

In this way, the mold for the casts assigned for the strength tests as well as the tester ATD10C-PŁ were prepared. The liquid metal was poured into previously prepared tester ATD10C-PŁ, which, differently from the conventional method, was also submerged in the water solution of Polihartenol-E8 (Fig. 2).
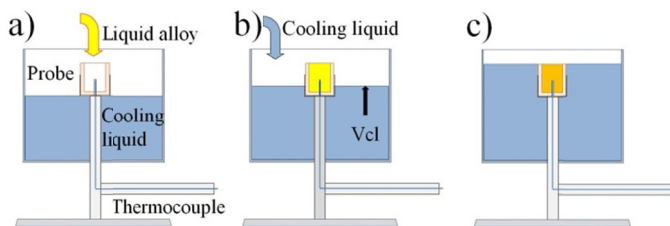

Fig. 2. Steps of alloy pouring (a) and intensive cooling of the TDA probe (b, c); V_{cl} = 0.08 m/s

The solidification time of 30% of the alloy volume in a random cast volume was determined with the use of simulation process by the MAGMA 5.3 software. Properties of the aluminum alloys were defined in the program based on the data from the MAGMA 5.3 system data base:
- alloy: AlSi7Mg,
- time of pouring the mold with the metal: 4 s,
- temperature of the liquid metal during pouring: 750°C,
- mold made of aluminum oxide: Al_2O_3,
- temperature of the ceramic mold: 150°C.

Evaluation of the following thermal processes of crystallization was performed by the TDA method: cooling ($t = f(\tau)$), kinetics ($dt/d\tau = f'(\tau)$) and dynamics ($d^2t/d\tau^2 = f''(\tau)$). On the derivative curve $dt/d\tau = f'(\tau)$, characteristic points were determined, which were then used to determine the thermal effects of crystallization for the selected alloy:

Y – temperature of the tester ATD10C-PŁ probes before pouring,

Z – maximum temperature of alloy after pouring into the TDA tester,

A-E – crystallization of primary phase α_{Al},

E-I – crystallization of eutectics $\alpha_{Al} + \beta(Si)$,

I-K – crystallization of phase $\alpha_{Al} + Mg_2Si + \beta(Si) + MM_{Mg2Si}$,

K-N – crystallization of phase $\alpha_{Al} + Mg_2Si + \beta(Si) + MM_{Al2Cu} + (MM_{AlSiCuNiFeMnCrVMoW})$

For description of the characteristic thermal effects occurring during primary crystallization, the quantities determined for the characteristic points were used:
- alloy temperature t,°C,
- value of the first derivative of temperature after time $dt/d\tau$,°C/s,
- time τ from the beginning of the measurement to the recording of a characteristic point on the derivation curve ($dt/d\tau$), s,
- value of the tangent of inclination angle of the straight line on the interpolar interval between the characteristic points $Z = \text{tg}(\alpha) \approx d^2t/d\tau^2$,°C/s².

In order to reveal the phases in the alloy's microstructure, the samples (micro-sections of the TDA probe) were etched in a 4% water solution of hydrofluoric acid. The metallographic tests were carried out by means of the optical microscope Nikon Eclipse MA200.

Examinations of the selected mechanical properties, i.e.: UTS, Elongation, were performed for samples of cylindrical casts, according to the standard EN-ISO 6892/1, by means of the testing machine Instron 4485. The HB hardness measurements were performed by the Brinell method with a 2.5 mm diameter steel ball, on the hardness tester KB Prüftechnik. The casting modulus of both types of castings (UTS, TDA) are different from each other. Differences of the casting modulus equal to about only 3% (M_{UTS} = 0.34 cm, M_{TDA} = 0.33 cm).

3. Discussion of the results

3.1. Microstructure of alloy AC-AlSi7Mg + cooled at ambient temperature and intensively cooled

Figure 3(a,b) shows the microstructure of alloys AC-AlSi7Mg + cooled in a ceramic mold at ambient temperature and intensively cooled, respectively. The alloy microstructure consists of the following phases: α_{Al} + eutectic (α_{Al} + β(Si)) + eutectic (α_{Al} + β(Si) + MM_{Mg2Si}) + eutectic (α_{Al} + β(Si) + MM_{Al2Cu}) + $MM_{AlSiCuNiFeMnCrVMoW}$. The additions of Cu, Ni, Cr, V, Mo and W introduced into the AC-AlSi7Mg alloy form complex non-equilibrium intermetallic phases (MM), such as: Mg$_2$Si (MM_{Mg2Si}), Al$_2$Cu (MM_{Al2Cu}) of different concentrations and combinations of the elements present in them alloy ($MM_{AlSiCuNiFeMnCrVMoW}$).

A very strong effect on obtaining microstructure without porosity defects, caused by the ceramic mold being penetrated by the water vapour, is exhibited by participation of the solid phase in the cast at the moment of initiation of intensive cooling of the mold. Performed simulations of process of pouring into ceramic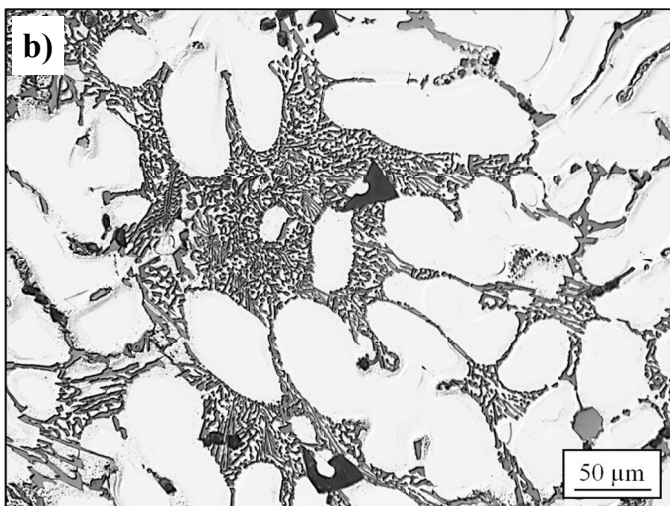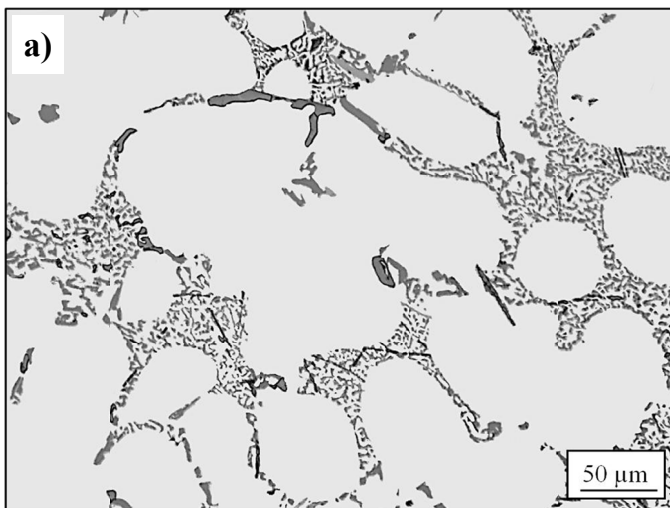 mold and alloy solidification, with the use of the MAGMA 5.3 software, as well as the validation of the simulation results under laboratory conditions made it possible to determine the time that should pass from the moment of pouring into mold to moment of submerging the mold in the cooling liquid. This time is necessary for formation of a solidified phase in the volume of the mold shaping the cast which is strong enough to withstand the pressure of the gases trying to get into the liquid alloy. Based on these tests, it was assumed that formation of a 30% solid phase in the alloy, in the area of the mold shaping the cast, makes it possible to obtain cylindrical casts without defects caused by porosity.

Figure 4 presents the simulation of the solidification process of the alloy in the ceramic mold which was used to determine time, calculated from the moment of filling the mold, after which the filled mold could be submerged in the cooling liquid without risk of the cast being gasified by the water vapour. In the volume of the cylindrical cast, after ca. 19.6 s from the moment of pouring into mold (Fig. 4), large areas were observed with about 30% of solid phase in the cast volume.
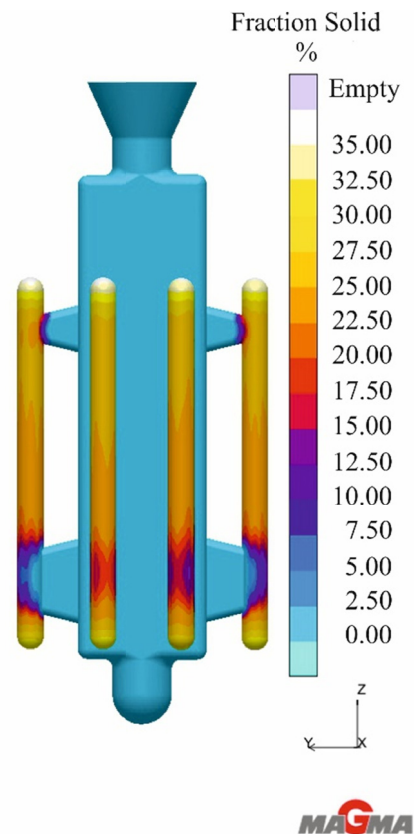

Fig. 3. Microstructure of AC-AlSi7Mg+ alloy: a) cooled at ambient temperature, b) cooled intensively

Fig. 4. Fraction of solid after 19.6 s (AC-AlSi7Mg)

3.2. TDA analysis

Figure 5 shows the characteristics of alloys AC-AlSi7Mg, solidifying in the TDA sampler at ambient temperature and cooled intensively in a water solution of the Polihartenol-E8.

Tables 1 and 2 present compilations of (t, $dt/d\tau$, $d^2t/d\tau^2$) determined for characteristic points or segments formed by these points ($Z \approx d^2t/d\tau^2$) from the TDA curves for the examined alloys.

TABLE 1

Characteristic points TDA for AC-AlSi7Mg+ alloy cooled
at ambient temperature

Point	τ, s	t, °C	$dt/d\tau$, °C/s	$d^2t/d\tau^2$, °C/s²	$Z = d^2t/d\tau^2 \cdot 10^{-3}$, °C/s²
Y	72.3	127.3	70.442	8.5257	—
Z	78.1	703.8	25.890	−14.3420	—
A	97.3	621.4	−2.414	0.1270	—
B	114.6	600.3	−0.270	0.0223	29.75
C	114.6	600.3	−0.270	0.0223	—
D	114.6	600.3	−0.270	0.0223	−18.56
E	266.9	549.3	−0.397	−0.0025	−4.48
F	289.3	543.9	−0.002	0.0211	12.93
G	299.5	544.8	0.144	−0.0026	—
H	321.3	546.4	−0.005	−0.0031	−7.81
I	466.6	523.6	−0.485	0.0002	−9.98
J	476.2	519.6	−0.330	0.0047	19.83
K	495.4	511.8	−0.496	−0.0009	−11.26
L	507.5	506.9	−0.239	−0.0003	29.24
M	507.5	506.9	−0.239	−0.0003	−43.84
N	528.0	495.5	−0.750	0.1381	−12.79

TABLE 2

Characteristic points TDA for AC-AlSi7Mg+ alloy cooled
intensively

| Point	τ, s	t, °C	$dt/d\tau$, °C/s	$d^2t/d\tau^2$, °C/s²	$Z = d^2t/d\tau^2 \cdot 10^{-3}$, °C/s²
Y	38.4	111.5	32.050	11.1576	—
Z	49.3	685.6	3.390	−5.6754	—
A	87.0	596.6	−1.416	0.0257	—
B	102.4	580.3	−0.558	0.0323	143.96
C	102.4	580.3	−0.558	0.0323	—
D	102.4	580.3	−0.558	0.0323	−42.66
E	167.7	527.2	−0.959	0.0122	−11.63
F	186.2	518.5	−0.004	0.0130	48.93
G	188.2	518.7	0.015	0.0032	—
H	190.1	518.6	−0.005	−0.0094	−31.33
I	219.5	506.6	−0.788	−0.0019	−36.66
J	226.6	501.2	−0.768	−0.0027	8.39
K	234.9	494.4	−0.928	−0.0271	−8.53
L	243.2	486.0	−1.081	−0.0320	—
M	243.2	486.0	−1.081	−0.0320	−82.56
N	264.3	449.0	−2.265	−0.0070	−12.38
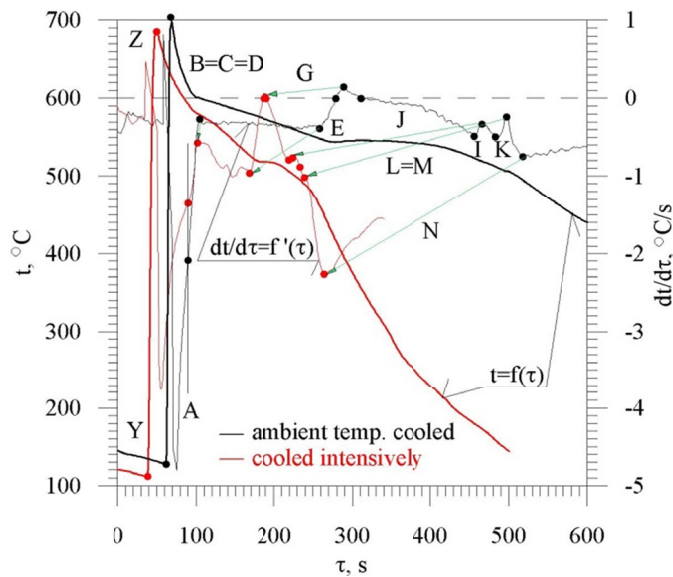
Fig. 5. Comparison of TDA characteristic for AC-AlSi7Mg+ alloy
cooled at ambient temperature and AC-AlSi7Mg + s cooled intensively

On the derivation curve ($dt/d\tau$), points A, B = C = D and E
determine the thermal effect of the crystallization of phase α_{Al} in
volume of the sampler: points E-I determine the thermal effect of
the crystallization of eutectic $\alpha_{Mg} + \beta$(Si), points I-K determine
the thermal effect of the crystallization of eutectics phase $\alpha_{Al} +$
$Mg_2Si + \beta$(Si) + MMMg$_2$Si, points K-N determine the thermal
effect of the crystallization of eutectics phase $\alpha_{Al} + Mg_2Si +$
β(Si) + MMAl2Cu + (MMAlSiCuNiFeMnCrVMoW). After
the alloy has been supercooled below the equilibrium liquidus
temperature, grains of phase α_{Al} nucleate and grow at the actual
liquidus temperature tA. The thermal effect A-B-C-D includes
the stage of intensive nucleation and growth of phase α_{Al}, whose
intensity drops on the segment between points D and E. At this
stage, before the crystallization front of phase α_{Al}, concentration

of Si slowly increases in the liquid alloy, which in consequence,
leads to nucleation and growth of eutectic $\alpha_{Al} + \beta$(Si). After the
metal has been supercooled below the equilibrium temperature of
eutectic transformation, at the actual transformation temperature
tF, eutectic $\alpha_{Al} + \beta$(Si) nucleates and grows. At this stage, before
the crystallization front of phase $\alpha_{Al} + \beta$(Si), the concentration of
Mg slowly increases in the liquid alloy, which leads to nucleation
and growth of eutectic $\alpha_{Al} + Mg_2Si + \beta$(Si) + MM$_{Mg2Si}$ between
points I and K. Finally between points K and N concentration
of other elements slowly increases in the liquid alloy, which
leads to nucleation and growth of eutectic $\alpha_{Al} + Mg_2Si + \beta$(Si)
+ MM$_{Al2Cu}$ + (MM$_{AlSiCuNiFeMnCrVMoW}$).

Alloy AC-AlSi7Mg+ solidifies in the volume of the
ATD10C-PŁ sampler at point N. Intensive cooling of alloy
AC-AlSi7Mg + s caused changes in kinetics and dynamics of
the thermal processes, as compared to the alloy solidifying at
ambient temperature, which in consequence, shortened the time
of nucleation of phase α_{Al} and growth of eutectic $\alpha_{Al} + \beta$(Si). Dif-
ference in the solidification time of the alloy within the volume
of the sampler between the alloy cooled at ambient temperature
and the one cooled intensively equals to $\Delta\tau_{A-N} = \tau_{A-N}$ ambient
$- \tau_{A-N}$ intensively = 253.4 s (faster by 58.83%), where the crystal-
lization time of phase α_{Al} shortened $\Delta\tau_{A-E} = \tau_{A-E}$ ambient $- \tau_{A-E}$
intensively = 88.9 s (faster by 52.42%) and the crystallization
time of the growth of eutectic $\alpha_{Al} + \beta_{Si}$ shortened $\Delta\tau_{E-I} = \tau_{E-I}$
ambient $- \tau_{E-I}$ intensively = 147.9 s (faster by 74.06%).

3.3. Strength properties UTS, Elongation and HB hardness

Table 3 presents mechanical properties UTS, A_t and HB
of alloys: AC-AlSi7Mg, AC-AlSi7Mg+ cooled at ambient tem-
perature and AC-AlSi7Mgs and AC-AlSi7Mg + s intensively

TABLE 3

Mechanical properties of alloys: AC-AlSi7Mg, AC-AlSi7Mg+
cooled at ambient temperature and AC-AlSi7Mgs
and AC-AlSi7Mg + s intensively cooled

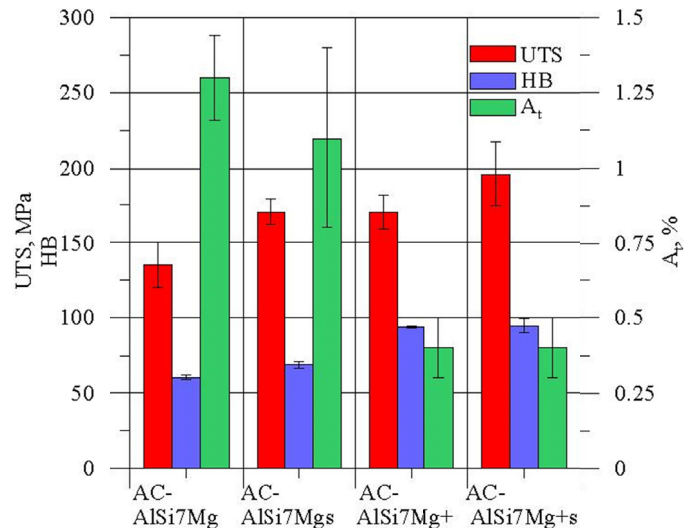| Alloy	UTS, MPa	Standard deviation, MPa	A_t, %	Standard deviation, %	HB, -	Standard deviation, -
AC-AlSi7Mg	135.0	14.79	1.3	0.14	60.0	1.47
AC-AlSi7Mg$_S$	170.1	8.50	1.1	0.30	68.5	2.20
AC-AlSi7Mg+	170.0	11.15	0.4	0.10	94.0	0.88
AC-AlSi7Mg + s	196.0	21.80	0.4	0.10	94.7	4.60

Fig. 6. Mechanical properties of alloys: AC-AlSi7Mg and AC-AlSi7Mg+ at ambient temperature cooled and cooled intensively: AC-AlSi7Mgs and AC-AlSi7Mg + s

cooled in a water solution of the Polihartenol-E8. Figure 6 shows a graphical presentation of these properties.

From the diagram (Fig. 6) it can be inferred that the refinement of the microstructure of intensively cooled alloys and the introduction of thermal stresses caused by the cooling process is the main reason for increase of UTS and HB of the examined alloys.

4. Conclusions

The following conclusions can be drawn from the studies of intensive cooling of the alloys without additions: AC-AlSi7Mg, as well as with Cu, Ni, Cr, Mo, V and W additions – AC-AlSi7Mg+ in a water solution of Polihartenol-E8:

- in reference to the crystallization:
  - intense cooling of the mold (TDA probe) caused a significant reduction in the crystallization time of the alloy respectively for:
    - primary solidification time $\Delta\tau_{A-N}$ faster by 58.83%,
    - crystallization time of phase α_{Al} $\Delta\tau_{A-E}$ faster by 52.42%,
    - crystallization time of the growth of eutectic α_{Al} + β(Si) $\Delta\tau_{E-I}$ faster by 74.06%,
- in reference to the microstructure:
  - for the examined alloys, both AC-AlSi7Mg and AC-AlSi7Mg+, a microstructure refinement was observed mostly of the primary phase α_{Al} and eutectic precipitations of phase β(Si),
- in reference to the mechanical properties:
  - the tensile strength UTS increase was observed (for alloy AC-AlSi7Mg by 26 %, for AC-AlSi7Mg+ by 15%),
  - the elongation At of the examined alloys was reduced (for AC-AlSi7Mg by 15 %, for AC-AlSi7Mg+ the elongation did not change),
  - the hardness of alloy AC-AlSi7Mg increased by 15%, and of alloy AC-AlSi7Mg+ by 0.7%.

REFERENCES

[1] F.C. Robles-Hernandez, J.M.H. Ramírez, R. Mackay, Al-Si Alloys: Automotive, Aeronautical, and Aerospace Applications, Springer (2017).

[2] E.R. Wang, X.D. Hui, S.S. Wang, Y.F. Zhao, G.L. Chen, Mater. Sci. Eng. A **527**, 7878-7884 (2010).

[3] M. Timpel, N. Wanderka, R. Schlesiger, T. Yamamoto, N. Lazarev, D. Isheim, G. Schmitz, S. Matsumura, J. Banhart, Acta Mater. **60**, 3920-3928 (2012).

[4] T. Szymczak, G. Gumienny, T. Pacyniak, Arch. Found. Eng. **16** (3), 109-114 (2016), DOI: 10.1515/afe-2016-0060.

[5] T. Szymczak, G. Gumienny, I. Stasiak, T. Pacyniak, Arch. Found. Eng. **17** (1), 153-156 (2017), DOI: 10.1515/afe-2017-0028.

[6] R. Władysiak, A. Kozuń, K. Dębowska, T. Pacyniak, Arch. Found. Eng. **17** (2), 137-144 (2017), DOI: 10.1515/afe-2017-0065.

[7] R. Władysiak, A. Kozuń, T. Pacyniak, Arch. Found. Eng. **16** (4), 175-180 (2016), DOI: 10.1515/afe-2016-0009.

[8] A. Eshaghi, H.M. Ghasemi, J. Rassizadehghani, Mater. Des. **32** (3), 1520-1525 (2011).

[9] B.P. Pisarek, C. Rapiejko, T. Szymczak, T. Pacyniak, Arch. Found. Eng. **17** (1), 137-142 (2017), DOI: 10.1515/afe-2017-0025.

[10] C. Rapiejko, B. Pisarek, T. Pacyniak, Arch. Metall. Mater. **62** (1), 309-314 (2017), DOI: 10.1515/amm-2017-0046.

[11] C. Rapiejko, B. Pisarek, E. Czekaj, T. Pacyniak, Arch. Found. Eng. **14** (1), 97-102 (2014). DOI: 10.2478/afe-2014-0022.